International Journal of Mass Spectrometry 293 (2010) 1–11

Contents lists available at ScienceDirect

International Journal of Mass Spectrometry

journal homepage: www.elsevier.com/locate/ijms

Proton transfer reactions of halogenated compounds: Using gas chromatography/Fourier transform ion cyclotron resonance mass spectrometry (GC/FT-ICR MS) and *ab initio* calculations

Indira K.C. Silwal, Jayendran C. Rasaiah *, Jan E. Szulejko, Touradj Solouki **

Department of Chemistry, 5706 Aubert Hall, University of Maine, Orono, ME 04469-5706, United States

ARTICLE INFO

Article history:
Received 31 July 2009
Received in revised form 9 March 2010
Accepted 13 March 2010
Available online 23 March 2010

Keywords:
Disinfection byproducts (DBP)
FT-ICR
Ab initio
Proton affinity (PA)
Entropy-driven

ABSTRACT

We combine modern GC mass spectrometric techniques (GC/FT-ICR MS) and *ab initio* molecular orbital calculations at G2, G3, and MP2/6-31+G** levels for characterization of disinfection byproducts (DBPs) present in treated drinking water samples. We introduce an additional dimension to GC/MS analysis that utilizes theoretically calculated proton affinities (PAs) and gas-phase basicities (GBs) to elucidate reaction mechanisms. The observed species at $m/z = 100.9$ (*i.e.*, $CH_3OCl_2^+$) in our GC/MS experiments is an ion-dipole complex ($CHCl_2^+ \cdots OH_2$), formally corresponding to protonated dichloromethanol (G3 calculated $PA_{CH_2OCl_2} \sim 163.3$ kcal mol^{-1}) produced in the gas phase either by the association of a water molecule with a $CHCl_2^+$ fragment ion from chloroform (present in the treated drinking water sample) or by the elimination of HCl in a condensation reaction between chloroform and protonated water. The calculated PA of chloroform at the G3 level ($PA_{CHCl_3} \sim 157.8$ kcal mol^{-1}) as well as entropy considerations indicate that a non-dissociative proton transfer (PT) reaction from H_3O^+ to $CHCl_3$ would be inefficient; however, the observed dissociative PT product ions (*e.g.*, $CHCl_2^+$) can be explained by considering the reaction entropy (ΔS). The overall dissociative PT reaction is unfavorable at 298 K and marginally exoergic ("entropy driven") under our experimental conditions at 360 K. Besides DBPs, we report the presence of the Zundel cation $H_5O_2^+$ in our mass spectrum. We speculate that the Zundel cation is formed by multiple ion-molecule reactions involving water in the presence of helium carrier gas and GC eluting compounds.

1. Introduction

During chemical disinfection of drinking water, disinfectants (chlorine, ozone, chlorinedioxide, chloramines) react with naturally occurring inorganic and organic substances that are present in the raw water and form disinfection byproducts (DBPs) [1,2]. Currently, approximately 600–700 DBPs have been identified [3,4]. The trihalomethanes (THM) such as chloroform, bromodichloromethane, dibromochloromethane, and bromoform are among the most routinely measured DBPs. Following the discovery of chloroform in chlorinated drinking water by Rook [5] and subsequent studies of its carcinogenic effects on animals [6], different epidemiological and laboratory studies have shown the adverse effects of DBPs on animals and humans (*e.g.*, colon and bladder cancers [7,8], low birth weight and fetal growth retardation [9,10]). After reports that DBPs such as bromate and halonitromethane damage deoxyribonucleic acid (DNA) in animal cells [11], DBPs and their associated adverse health effects became important topics of public concern. The exact toxicity of some DBPs, such as chloroform, at the levels present in drinking water have not been decisively established [12].

Gas chromatography/mass spectrometry (GC/MS) [4,13,14], and liquid chromatography/mass spectrometry (LC/MS) [4,15,16] have been widely employed to identify DBPs. More recently, electrospray ionization mass spectrometry (ESI MS) [17] was used to identify different polar DBPs. In conventional GC/MS experiments, mass spectrometric patterns (the types and relative abundances of parent and fragment ions observed in the mass spectrum), and to a less extent analyte retention times (RTs), are used for unknown identification. The retention time and analyte elution order depend on a number of GC experimental variable parameters and hence, analyte identifications by GC/MS often rely on mass spectrometric data only [18].

Previously, we used GC/FT-ICR MS to detect potential DBPs using electron impact ionization (EI); identifications were confirmed by comparisons of MS patterns using authentic chemical standards

* Corresponding author. Tel.: +1 207 581 1179; fax: +1 207 581 1191.
** Corresponding author. Tel.: +1 207 581 1172; fax: +1 207 581 1191.
E-mail addresses: rasaiah@maine.edu (J.C. Rasaiah), solouki@maine.edu (T. Solouki).

1387-3806/$ – see front matter © 2010 Elsevier B.V. All rights reserved.
doi:10.1016/j.ijms.2010.03.003

[19]. However, the EI technique leads to extensive fragmentation of DBPs and can yield mass spectra with very little or no trace of molecular ions. The fragmentation pattern and mass spectrometry database libraries can be used to assign an identity for an unknown DBP but there may still be uncertainty over the validity of this assignment. For example, MS data for a "true unknown" may not even be available in commercial MS library databases. Hence, it is important to have additional methods of analyses that can provide complementary structural or thermochemical information [20] for unknown identification. For example, functional group specific ion-molecule reactions, determination of the gas phase basicity (GB), or PA of an analyte, concurrent with its GC/MS analysis can in principle provide additional dimensions to improve GC/MS analysis [21,22]. In this context, we note that Munson and co-workers reported the use of reactant ion monitoring (RIM) [23] and PA bracketing [24] to determine analyte quantity and ion thermochemistry, respectively. This approach was extended for simultaneous determination of analyte concentration, gas phase basicities, and proton transfer (PT) kinetics with GC/FT-ICR MS [21].

In this study, we carried out GC/FT-ICR MS experiments with EI, chemical ionization (CI), and *ab initio* calculations of PAs and GBs to characterize DBPs in drinking water [19]. Furthermore, we used multiplexed RIM (MRIM) of the CI reagent ions (R_iH^+) [21,22] to bracket the gas phase basicities of the neutral analytes eluting from the GC column. In the PA bracketing approach [21], the degrees of CI reactant ion depletions can be monitored in a single GC/FT-ICR MS experiment to obtain thermochemical data for GC eluting analytes. The application of this method to DBPs (using reference conjugate bases with coarse PA steps) yielded reagent ion dependent bracketing results with limited accuracy for gas-phase basicity measurements, highlighting the importance of reaction entropy. Here we show the importance of entropy considerations and the combined use of theoretical calculations with experimental ΔG measurements to elucidate PA and ion-molecule reaction mechanisms. This method adds another dimension to the MS analysis of DBPs, which can be extended for analysis of other unknowns.

2. Experimental

2.1. Instrumentation

All experiments were performed using a 7-T FT-ICR MS (Ion Spec Corp., Forest Lake, CA) equipped with an in-house designed GC interface [21,22]. The SRI model 8610C GC and an in-house configured cryofocuser were interfaced with FT-ICR MS (based on Jacoby and co-workers' design [25]). A 105-m (0.25-mm i.d., 1-μm crossbonded 100% dimethyl polysiloxane stationary phase coating) MXT-1 capillary column (Restek Corp., Bellefonte, PA) was used for all solid phase microextraction (SPME) GC experiments [19]. The vacuum chamber surrounding the ICR cell was maintained at ~87 ± 5 °C (360 ± 5 K) by a set of DC heating elements [26].

2.2. GC Programming

The GC programming for all SPME experiments was as follows: the initial temperature was set at 40 °C and held for 4 min to park the desorbing species at one end of the GC column close to the injection port (maintained at 160 °C), then ramped at 5 °C per minute to 180 °C and finally kept isothermal at 180 °C for 12 min. The carrier gas (He) head pressure was set at 15 psi.

2.3. Chemicals and sample preparation

Standard reagents such as methanol and chloroform were purchased from commercial sources (Sigma–Aldrich Chemical Company, Inc.) and used without further purification. Headspace SPME sampling technique was used to extract potential disinfection byproducts from drinking water samples [27,28]. Specifically, 20 mL of drinking water sample and a magnetic stirring bar were placed in a 40-mL EPA septum sealed vial. The 85 μm Carboxen/PDMS Stableflex™ fiber (Supelco-Bellefonte, PA) was exposed to the water sample for 30 min, and retracted and inserted into the injection port for GC/FT-ICR MS analysis.

2.4. Introduction of chemical ionization reagents

A 250-mL reservoir connected to a pulsed valve contained the CI reagent mixture of water and methanol (a ~1:1 molar ratio) at a pressure of ~1 Torr. Liquid nitrogen was used for conventional freeze-pump-thaw degassing cycles (to freeze the organics) and remove the air from the CI reagent mixture. After the quench event (which is used to remove ions from the ICR cell), water and methanol from the reservoir were pulsed into the ICR cell (for 3 ms or t = 0–3 ms). After a short delay of ~400 ms (t ~ 3 to 400 ms) water and methanol reagents were ionized by 70 eV electrons for 1000 ms (t = 400–1400 ms). A reaction delay (of ~5100 ms) was used to generate the chemical ionization (CI) reagent ions. The reagent ions were isolated (at t = 6000–6032 ms), using stored waveform inverse Fourier transform (SWIFT) [29,30], prior to the GC effluent introduction (t ~ 6500 ms) *via* a separate pulsed valve cyrofocusing assembly [21]. Excitation/detection events and recording of the time-domain signal occurred ~8500 ms after the GC effluent introduction. Fourier transformation of the resulting time-domain signals (256 k data points) with one zero-fill, baseline correction and Hamming apodization followed by magnitude calculation, and frequency-to-mass conversion yielded the GC/FT-ICR mass spectra. All mass spectra were constructed from a single time-domain data set.

2.5. Kinetic schemes

The MRIM approach [21] was used to calculate the gas-phase basicities (GB) of analytes. Experiments were performed under the presumed condition that the GC eluting analyte concentrations were in excess of the concentration of reagent ions; hence, the ion-molecule reactions were assumed to be pseudo first order [31]. The proton transfer (PT) reaction efficiencies can be determined by measuring the minimum normalized abundance (ε_{ij}) of the ith reactant ion with the jth GC eluting analyte [21]. For example, the ion abundance ratio of the remaining reagent ion (at the maximum reagent ion depletion "$[R_iH^+]_t$") to total reagent ion before analyte elution (*i.e.*, before the consumption of any reagent ions "$[R_iH^+]_0$") is ε_{ij} (Eq. (1)):

$$\varepsilon_{ij} = [R_iH^+]_t/[R_iH^+]_0 \quad (1)$$

and PT from chemical ionization reactant ions (R_iH^+) to GC eluting analyte (A_j) in an ICR cell (Eq. (2)) can be determined by using MRIM method [21]:

$$R_iH^+ + A_j \rightarrow R_i + A_jH^+ \quad (2)$$

For the experiments reported here, the ε_{ij} value for H_3O^+ reagent ion (the ion with the highest acidity corresponding to the conjugate base [51] with the lowest PA) can be used as the reference to calculate PT and other ion-molecule reaction efficiencies for reactant ions; H_3O^+ reagent ion showed the maximum depletion among the three reagent ions used in this study. For an exoergic PT reaction, the PT reaction rate k_{ij} can be assumed to be near the Langevin collision rate constant (k_{Lg} or maximum ion-molecule collision rate constant, *i.e.*, $k_{ij} = k_{Lg}$) which corresponds to every collision leading to formation of product(s). For the particular reactions discussed herein, the ε_{ij} value of H_3O^+ was used as the reference depletion value (ε_{coll}) and we assumed that the analyte reaction with H_3O^+

Table 1
Summary of SPME GC/FT-ICR MS results.

Retention time (min)	Experimental m/z value	Theoretical m/z value	MME (ppm)	Elemental composition	Potential parent molecule (observed product ions)
20.0	129.9140	129.9138	~2	$C_2H^{35}Cl_3^+$	($[C_2HCl_3]^{\bullet+}$)
20.0	116.9066	116.9060	~5	$C^{35}Cl_3^+$	$CHCl_3$ ($[M-H]^+$)
20.0	82.9446	82.9450	~5	$CH^{35}Cl_2^+$	$CHCl_3$ ($[M+H-HCl]^+$)
20.0	46.9683	46.9683	~0	$C^{35}Cl^+$	$CHCl_3$ ($[M+H-2HCl]^+$)
20.7	100.9559	100.9556	~3	$CH_3O^{35}Cl_2^+$	$CHCl_2OH$ ($[M+H]^+$)
20.7	82.9446	82.9450	~5	$CH^{35}Cl_2^+$	$CHCl_2OH$ ($[M+H-H_2O]^+$)
20.7	64.9784	64.9789	~8	$CH_2O^{35}Cl^+$	$CHCl_2OH$ ($[M+H-HCl]^+$)

$CHCl_3$ = chloroform; $CHCl_2OH$ = dichloromethanol (presumably, if it were present in water samples).

occurred at the Langevin collision rate. This assumption is valid for exoergic [33,34] PT reactions (*e.g.*, H_3O^+ + analyte → product(s)) that have no forward activation barriers. The information about PT reaction efficiency (η_{ij}) of DBPs (analyte) is extracted from the selected ion chromatogram (SIC). The GB of an eluting GC analyte (A_j) can be determined from the thermokinetic method developed by Bouchoux et al. [34] in which the PT reaction efficiency ($\eta_{ij} = k_{ij}/k_{Lg} = \ln(\varepsilon_{ij})/\ln(\varepsilon_{coll})$) [21] is related to the PT reaction Gibbs free energy change (*i.e.*, $\Delta G_{ij} = GB(R_i) - GB(A_j)$) as in Eq. (3):

$$GB(A_j) = GB(R_i) + RT \times \ln(1/\eta_{ij} - 1) \quad (3)$$

3. Computational details

Standard *ab initio* molecular orbital calculations were performed with Gaussian 03 programs [35]. The MP2/6-31+G** basis set was used for the geometry optimization and total energy calculations for all reactions. In addition, the energy of each species was calculated at the G2 level [32] with geometry optimization at MP2/6-31G(d) level. The energies of chloromethanes (CH_3Cl, CH_2Cl_2, and $CHCl_3$ but excluding CCl_4), two of the chloromethanol series (CH_2ClOH, $CHCl_2OH$), and chloromethyl hypochlorite $ClCH_2OCl$, which is an isomer of dichloromethanol, were also calculated at the G3 level [36]. In the G2 and G3 procedures, the zero point energy correction was from HF/6-31G (d) frequencies scaled with standard scaling factor of 0.8929 [37,38]; this allowed us to compare our results with the previously reported values [39–42]. Ma et al. [39] have noted the differences between MP2 and HF structures/frequencies as a starting point for higher level calculations and mention that MP2 yields improved total energies for radical cations but the differences are insignificant for neutrals.

PAs were determined by direct *ab initio* calculations of the differences in the energies of the protonated (BH^+) and unprotonated (B) species at the G3 level of theory [32,36,39,43,44] at 298 K. PA is the negative of the enthalpy change ΔH for the gas-phase protonation reaction (Rx) of the base B, ($B + H^+ = BH^+$) from which it follows that

$$PA(B) = -\Delta H_{Rx} = H_T(B) - H_T(BH^+) - 5/2RT,$$

Table 2
Calculated G3 energies (hartrees) and proton affinities (kcal mol^{-1}) of selected chloromethanes and selected chloromethanols.

Species	Calculated G3 energies		Calculated G3 PA		Experimental PA
	G3 (0 K)	G3 (298 K)	PA_0	PA_{298}	PA_{298}
CH_3Cl	−499.913022	−499.909987 (−499.911500)[a]	153.9	154.8 (155.2)[a] (154.9)[c] (155.4)[d] (154.7)[h]	154.7[b]
CH_4Cl^+	−500.158214	−500.154317			
CH_2Cl_2	−959.371216	−959.367633 (−959.370230)[a]	151.0	151.1 (150.7)[a] (151.0)[e] (153.5)[f] (149.8)[h]	150.2 ± 2.0[g]
$CH_3Cl_2^+$	−959.611860	−959.606081			
$CHCl_3$	−1418.828848	−1418.824384 (−1418.828320)[a]	158.0	157.8 (158.2)[a] (157.8)[h]	
$CH_2Cl_3^+$	−1419.080649	−1419.073518			
CH_2ClOH	−575.095581	−575.092181	171.0	172.0	
$CH_2ClOH_2^+$	−575.368043	−575.363873			
CH_2ClOCl	−1034.491801	−1034.487041	161.2	162.4	
$CH_2Cl(OH)Cl^+$	−1034.748595	−1034.743386			
$CHCl_2OH$	−1034.564106	−1034.559599	162.2	163.3	
$CH_2Cl_2OH^+$	−1034.822517	−1034.817465			

Numbers in parenthesis are theoretical values from the literature.
[a] From Ref. [39].
[b] From Ref. [51].
[c] From Ref. [41].
[d] G2 calculation from Ref. [42].
[e] CCSD(T) calculations Ref. [56].
[f] B3LYP calculations Ref. [56].
[g] Experimental value from Ref. [56].
[h] From Ref. [49].

where $5/2RT$ is the ideal gas enthalpy of the hydrogen ion at temperature T. The enthalpy difference $H_T(B) - H_T(BH^+)$ can be replaced by the energy difference $E_T(B) - E_T(BH^+)$ since the PV term in the definition of the enthalpy $H = E + PV$ cancels out. The energy $E_T(X) = E_0(X) + E_{Therm}(X)$, where the last term is the thermal correction to the energy at finite temperature from vibrational and rotational degrees of freedom, was calculated using the standard expressions for the partition function for these modes of motion [45]. The energy $E_0(X)$ at 0 K is the electronic energy with the zero point energy correction added after scaling as described above. Summary of the SPME GC/FT-ICR MS and G3 calculations are presented in Tables 1 and 2, respectively. To our knowledge, the PAs of the CH_2ClOH and $CHCl_2OH$ have not been previously reported, although Phillips et al. [46] have reported calculations of the energies of the neutral $CHCl_2OH$ at the MP2 level using the 6-31+G** basis set. In addition, our results for the energies and PAs of CH_3Cl, CH_2Cl_2, and $CHCl_3$ are in good agreement with previous work except as noted in the next section.

The PAs and gas phase basicities (GBs) of the two chlorinated compounds of interest in our experimental study, namely chloroform and dichloromethanol, were also calculated at 298 K and at the temperature of our experiments (360 K). The gas-phase basicity (GB), which is the negative of the free energy change ΔG for the protonation reaction, and proton affinity (PA) are related by

$$GB = PA + T[\Delta S^T_{1/2} - S^T_{(H+)}]$$

where T is the temperature in kelvin, $\Delta S^T_{1/2}$ is the entropy difference between protonated and unprotonated species and $S^T_{(H+)}$ is the gas-phase entropy of the hydrogen ion. The entropies of the hydrogen ion, calculated from the Sackur–Tetrode equation [47] at 1 atm pressure are $S^{360}_{(H+)} = 26.9\,cal\,K^{-1}\,mol^{-1}$ and $S^{298}_{(H+)} = 26.0\,cal\,K^{-1}\,mol^{-1}$ [20,34].

4. Results and discussion

Various analytes such as bromodichloromethane, dichloromethane, dichloroacetonitrile, ethanol, mercaptans, and trichloropropanone were present at low concentrations in a local town's treated water samples and accurate mass measurement (MMA) analysis allowed their confident characterization [19]. However, the most abundant GC peak (RT range of 19.5–21.5 min) displayed a wider peak width and was originally assigned to two co-eluting compounds (*viz.*, chloroform and tentatively dichloromethanol) [19]. This work is focused on detailed characterization of the GC peak in the retention time range of 19.5–21.5 min. The ion molecule reactions reported herein were carried out at 360 K (the temperature of the vacuum chamber) assuming no thermal decomposition of analytes during the sample elution from the GC injection port to the ICR cell. We show that the combined use of experimental data and theoretical calculations allows confident characterization of the gas-phase reaction mechanisms.

The results of SPME analyses of a treated drinking water sample (from a local town in Maine) [19] for retention time range of 19.5–21.5 min are summarized in Table 1. Conventional FT-ICR mass calibration [21,22] (using five external calibrants) was used to calibrate the mass scale and yield average MMA below 5 ppm in the mass range of m/z = 15–450 for the reported data.

Columns one through six, in Table 1, contain the observed retention times (RTs), mass-to-charge (m/z) values (experimental and theoretical), mass measurement errors (MME) in parts per million (ppm), assigned elemental compositions, and potential parent molecules corresponding to the major components present in the analyzed sample. To reduce the size of Table 1, we have only included MS data for representative species corresponding to the most abundant natural isotopomers (*e.g.*, compositions with ^{79}Br, ^{12}C, ^{35}Cl, ^{1}H, ^{14}N, ^{16}O).

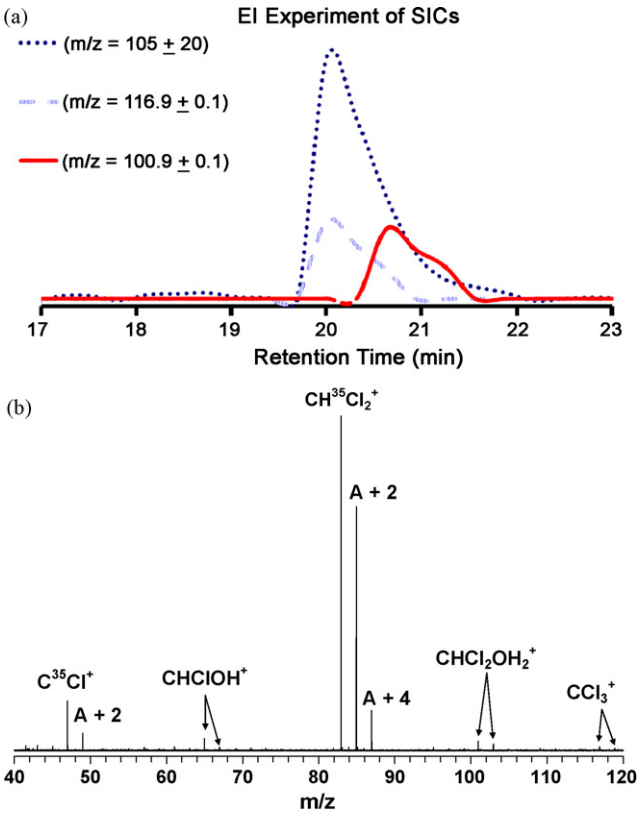

Fig. 1. (a) Selected ion chromatogram of wider mass range (m/z = 105 ± 20) and GC eluted compounds: CCl_3^+ (m/z = 116.9) from chloroform and supposed dichloromethanol $CHCl_2OH_2^+$ (m/z = 100.9). (b) EI mass spectrum of GC eluted compounds: suspected dichloromethanol and chloroform at the same retention time. "A" represents the isotope peak containing all the lowest nominal mass isotopes (^{12}C, ^{35}Cl) and A + n (n = 2, 4) designates isotopic peaks n nominal mass units heavier than the "A" peak.

Fig. 1a contains three selected ion chromatograms (SICs) from 70 eV EI GC/FT-ICR MS for m/z 100.9 ± 0.1, 116.9 ± 0.1, and a wider mass range of 105 ± 20. In Fig. 1b, the EI (70 eV) FT-ICR mass spectrum corresponding to retention time (RT = 20.0 min) is shown. Centroids for the two different retention times (dashed line around RT = 20.0 min, and solid line around RT = 20.7 min) of selected ion chromatograms in Fig. 1a suggest the presence of two compounds; presumably, chloroform at RT = 20.0 min, and an unknown compound with the elemental composition of protonated dichloromethanol ($CHCl_2OH_2^+$) at RT = 20.7 min. In other words, the mass spectrometric pattern variations across RT ~19.5–21.5 min, low pseudo molecular ion abundances, and potentially observed common fragment ion ($CHCl_2^+$) resemble elution of two distinct compounds and make analyte characterization difficult. For example, one might assign the peak centroids for m/z 116.9 ($[CCl_3]^+$) and 100.9 ($[CH_3OCl_2]^+$) at retention times of ~20.0 and ~20.7 min to two different compounds (*e.g.*, $[M-H]^+$ of chloroform and $[M+H]^+$ of dichloromethanol). Additional experiments were performed to confirm the identities of these species. Previously, we showed that PAs could be used to differentiate between isomers and structurally similar compounds eluting from a GC column [21,22]. We had originally noted that the utility of PA as an additional analysis dimension required consideration of all competing reactions [21,22] and entropy considerations. Here we methodically show that competing pathways such as "dissociative proton attachment (DPA)" and condensation reactions in conjunc-

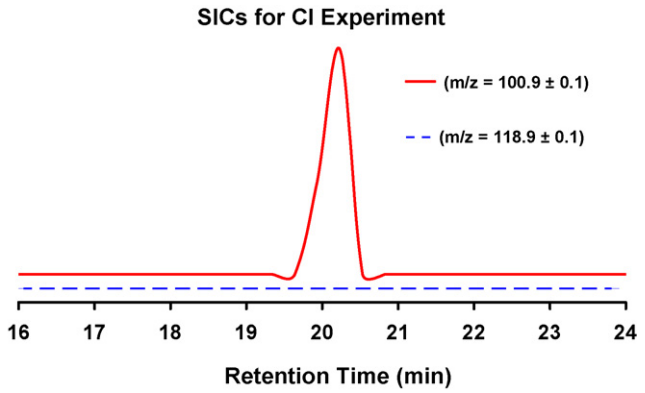

Fig. 2. Selected ion chromatograms (SIC) of $m/z = 100.9$ (suspected dichloromethanol) and $m/z = 118.9$ ($H_2CCl_3^+$ $[M+H]^+$ of chloroform) after proton transfer reaction from protonated water (H_3O^+).

tion with high level *ab initio* calculations can be used to elucidate ion-molecule reactions.

Three chemical ionization (CI) reagent ions covering the range of conjugate base (R_i) proton affinities (PAs) from ~165 to ~180 kcal mol^{-1} were selected to monitor PT reactions with the GC eluting analytes. Specifically, the CI reagent ions were generated by EI/self-chemical ionization (SCI) of water and methanol to SWIFT isolate [29,30] reagent ions (H_3O^+, CH_2OH^+, and $CH_3OH_2^+$) inside an ion cyclotron resonance (ICR) cell. If PT from the reagent ions to the GC eluting analytes occurs, the protonated analyte species should be observed in the SIC of the eluting analytes (as seen in Fig. 2).

The selected ion chromatograms of $m/z = 100.9$ (presumably protonated dichloromethanol) and $m/z = 118.9$ ($[M+H]^+$ of chloroform if formed) in *the CI* mode are shown in Fig. 2. The absence of a peak at RT ~20 min for SIC of m/z 118.9 (*i.e.*, $CH_2Cl_3^+$) indicates that there is either no PT from the protonated CI reagent water (PA of 165 kcal mol^{-1}) to the GC eluting analyte or the protonated product is unstable. This suggests that either (a) the PA and/or GB of chloroform, which have not been reported experimentally, are lower than the PA and GB of water or (b) the protonated chloroform is unstable in the ICR time scale of ms to s. Presumption of lower PA and/or GB values for chloroform is in agreement with the theoretical results of Ma et al. [39] and the experimental findings of Španěl and Smith [48] who tried the same PT reaction (under "thermal energies") in a selected ion flow tube studies and observed only a low efficiency (~3% reaction efficiency) clustering reaction for formation of $CH_3Cl\cdots H_3O^+$ with a branching ratio of 100%.

To characterize the observed species at $m/z = 100.9$, which coincidentally has the same m/z as protonated dichloromethanol, we note that its presence indicates that either (a) dichloromethanol has a GB value greater than GB_{H2O}, and/or (b) possible ion-molecule reaction(s), *e.g.*, hydronium ions with chloroform, yields this product ion at m/z 100.9. We carried out an MRIM experiment [21] to investigate the ion-molecule chemistry. Hence, three CI reagent ions (R_iH^+): protonated water (H_3O^+), protonated formaldehyde (CH_2OH^+) and protonated methanol ($CH_3OH_2^+$), were selected to bracket the gas phase basicities (GB) of the neutral analytes eluting from the GC column. When the eluting analytes exit the GC/MS interface and enter into the ICR cell the total reagent ion abundance can be attenuated [21] (for example, see Fig. 3a). The attenuations in Fig. 3a could be due to ion-molecule reactions, in particular PT reactions from the CI reagent ions to the GC eluting analytes. The individual reactant ion chromatograms ($m/z = 19$, 31, and 33) are shown in Fig. 3a and the mass spectrum corresponding to the RT ~20 min is shown in Fig. 3b. The depletion of the other two reagent ion at m/z 31 and 33 (the conjugate acids of the bases with

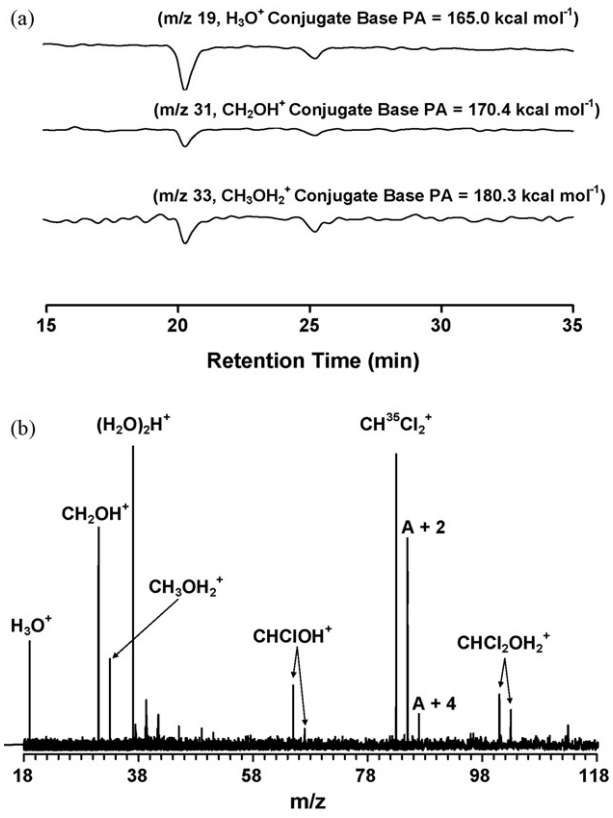

Fig. 3. (a) Reactant ion monitoring (RIM) chromatograms showing depletions of selected reagent ions (protonated water; H_3O^+, O protonated formaldehyde; CH_2OH^+ and O protonated methanol; $CH_3OH_2^+$) by analyte ($m/z = 100.9$ at RT = 20.7 min). (b) Mass spectrum of analyte ($m/z = 100.9$ and including remaining reagent ions) corresponding to RT = 20.7 min.

PA values at ~170 and ~180) were also observed. Depletions of the SICs from m/z 19, 31, and 33 are ~69%, ~23%, and ~33%, respectively. The MRIM results for PA determination of an analyte and bracketing approach (neglecting the: (a) potential entropy contributions, (b) activations barriers, and/or (c) alternative reaction channels) should be internally consistent and reagent ion independent. However, the use of simple PA bracketing approach for the data in Fig. 3 yields CI reagent ion dependant PA values and suggests the availability of other reaction channels. For example, the depletion of reagent ions at m/z 31 and 33 could be due to ion molecule reactions other than proton transfer reactions. Likewise, the reagent ion at m/z 19 (hydronium ion, H_3O^+) could react with chloroform to yield protonated chloroform and water, and the estimated ΔG for this reaction at 360 K is slightly endoergic but dissociation to fragment ion ($CHCl_2^+ + H_2O + HCl$) is exoergic by ~−0.2 kcal mol^{-1}.

The dissociation of protonated chloroform to give $CHCl_2^+ + HCl$ is exoergic (at 360 K) by approximately −0.6 kcal mol^{-1}; this ΔG value is estimated by using a ΔH value of approximately 6.0 kcal mol^{-1} from reference [49] and the entropy estimate of 18.2 cal mol^{-1} K^{-1} (based on the present G3 calculations for protonated chloroform, $CHCl_2^+$, and HCl). Also, to calculate the ΔG value for the reaction of chloroform with hydronium ion (discussed above) we used the NIST data [51] (*i.e.*, entropy and PA for water, and entropy for hydronium which was approximated to its isoelectronic analogue (ammonia)). Similarly, the reaction of H_2COH^+ with chloroform to give protonated dichloromethanol, HCl, and H_2CO is estimated to be mildly endoergic ($\Delta G_{360} = 0.6$ kcal mol^{-1}) and may be observed experimentally. Furthermore, the reaction of $CH_3OH_2^+$ with chloroform to give protonated dichloromethanol, HCl, and

CH_3OH is estimated to be endoergic ($\Delta G_{360} = 3.3$ kcal mol^{-1}) and may be observed in our SPME/GC/FT-ICR MS experiments. These entropy driven reactions may be further enhanced by a blackbody infrared radiative dissociation (BIRD) type mechanism [50].

The normalized SICs of the reactants in Fig. 3a are placed in an ascending order from top to bottom on the basis of the PA values of their conjugate bases [51]. Among the three reagent ions, the conjugate base of $CH_3OH_2^+$ (bottom trace in Fig. 3a) which is methanol (CH_3OH), has the highest PA (180.3 kcal mol^{-1}). The degree of depletion (at RT = 20.7 min) is maximum for H_3O^+ and less for CH_2OH^+ and $CH_3OH_2^+$. Based on the observed depletion of all reagent ions with the appearance of presumed protonated dichloromethanol ($m/z = 100.9$), it can be concluded that either (a) the PA of the analyte that yields $m/z = 100.9$ is higher than 180.3 kcal mol^{-1}, (b) there are alternative reaction channels to form 100.9 (formally, protonated dichloromethanol) with all three reagent ions, or (c) reaction is exoergic but "entropy driven" for analytes that have lower PA values than the conjugate base of the consumed reagent ion(s). It could be hypothesized that the observed ion at $m/z = 100.9$ is protonated dichloromethanol. However, as mentioned earlier in this section, the experimentally determined gas phase basicity (GB) of the unknown analyte (conjugate base corresponding to the protonated ions at $m/z = 100.9$) appeared to be reagent dependent, and hence suggested the existence of alternative potential condensation pathways for product formation. Based on the observed $m/z = 100.9$, dichloromethanol is a possible candidate for the unknown halogenated compound in the water sample. However, a literature search shows that dichloromethanol is unstable in water [46]. The presence of multiple peaks including the protonated water dimer $(H_2O)_2H^+$, $CHClOH^+$, and $CHCl_2OH_2^+$ in the mass spectrum (Fig. 3b) led us to suspect that the $m/z = 100.9$ peak could be due to ion molecule reactions [48] other than proton transfer reaction to dichloromethanol. Our observations (see Fig. 3b) are analogous to the consecutive losses of HCl from protonated 1,1-dichloroethane to give $CH_3CHClOH_2^+$ and CH_3CHOH^+ reported by Španěl and Smith [48].

To determine the identity of the species at m/z 100.9, we carried out an experiment with an authentic sample of chloroform in de-ionized water and observed the same $(CHCl_2OH_2)^+$ ion of $m/z = 100.9$ in the mass spectrum of the authentic sample as in the local water sample containing $CHCl_3$ and other DBPs. Trace amounts of water from using SPME and/or cryofocuser type GC/FT-ICR MS interface can influence the observed mass spectrometric patterns and the reported ion molecule reactions of chloroform are relevant to such experiments. This suggested that the $(CHCl_2OH_2)^+$ was an ion-dipole complex $(CHCl_2\cdots OH_2)^+$ generated in the gas-phase and not protonated dichloromethanol formed by non-dissociative proton transfer reactions. The complex could be formed in several different ways (see schemes I, II, and III) – by the elimination of HCl directly (I) or through the formation of an ion-dipole complex [52–54] from the condensation of chloroform with protonated water (II) in the ICR cell as shown below:

$$H_3O^+ + CHCl_3 \rightarrow [CHCl_2\cdots OH_2]^+ + HCl \quad (I)$$

$$H_3O^+ + CHCl_3 \rightarrow [CHCl_3\cdots H_3O]^+ \rightarrow [CHCl_2\cdots OH_2]^+ + HCl \quad (II)$$

For scheme I and II, we calculated, at the G2 level, an exothermicity of about 5 kcal mol^{-1} (see Table 4) supporting the experimentally observed chemistry. A third possibility is the association reaction (III) of one of the fragment ions of chloroform *i.e.*, $CHCl_2^+$ at m/z 82.9 and background water as discussed previously in a different context by Marotta et al. [55].

$$CHCl_2^+ + H_2O \rightarrow [CHCl_2\cdots OH_2]^+ \quad (III)$$

The presence of the species at $m/z = 64.97$ (*i.e.*, CH_2OCl^+) which contains only one chlorine atom (Fig. 3b) could be the result of HCl elimination from the ion-dipole complex of $[CHCl_2\cdots OH_2]^+$ to form $[CHClOH]^+$ (formally protonated chloroformaldehyde):

$$[CHCl_2\cdots OH_2]^+ \rightarrow [CHClOH]^+ + HCl$$

This agrees with the findings of Španěl and Smith [48], and Marotta et al. [55]. A qualitative comparison of the PA for chloroform using Hess law and NIST thermochemical data for neutrals (*e.g.*, $CHCl_3$ and HCl), appearance energy values for respective ions ($CHCl_2^+$, H^+), stationary electron convention (*i.e.*, heat of formation for electron is taken as zero at all temperatures), and a typical ion-dipole complexation energy of −10 kcal mol^{-1} [52] reconfirmed that chloroform's PA is lower than water. For more accurate PA determinations we used high level *ab initio* calculations. The details are provided in the following section(s).

To confirm and determine the "true" identity of the unknown at $m/z = 100.9$ we carried out *ab initio* computational studies to investigate the following:

(i) The gas phase reaction between neutral dichloromethanol $CHCl_2OH$ and a water molecule.
(ii) Proton transfer reactions between dichloromethanol and chloroform with protonated water.
(iii) The condensation reaction of chloroform with protonated water.
(iv) The association reaction of $CHCl_2^+$ and neutral water.

ab initio investigations of the gas phase reaction of neutral dichloromethanol ($CHCl_2OH$) with one neutral water molecule show that dichloromethanol reacts with water to form ClCHO, H_2O, and HCl. This was shown independently by us and earlier by Phillips et al. [46].

$$CHCl_2OH + H_2O \rightarrow ClCHO + H_2O + HCl$$

We confirmed that the activation barrier for water-catalyzed decomposition of $CHCl_2OH$ is 20.5 kcal mol^{-1}, and that the reaction is exothermic by 5.1 kcal mol^{-1}. Phillips et al. [46] have shown that the activation barrier for this reaction decreases as the number of water molecules is increased (Fig. 6b in Ref. [46]). It is observed that the proton is transferred from dichloromethanol to a water molecule. This is followed by bond formation between a chlorine atom that leaves the dichloromethanol and the hydrogen atom that leaves the protonated water to form neutral HCl with the release of a neutral water molecule. These calculations suggest that treated water samples do not contain dichloromethanol as it is hydrolytically unstable.

We next studied the PA of dichloromethanol, its isomer (hypochlorite), and the chloromethane series (chloromethane, dichloromethane, and trichloromethane {chloroform}). The calculated G3 total energies and the corresponding PAs of the selected chlorinated species at 298 K are presented in Table 2. It is interesting that the PA values of the chloromethane series (chloroform, dichloromethane and chloromethane) do not change linearly and monotonically with the number of substituted chlorine atoms as expected from simple additivity considerations. The PA decreases from chloromethane (153.9 kcal mol^{-1}) to dichloromethane (151.0 kcal mol^{-1}) and then increases on further chlorination to chloroform (158.0 kcal mol^{-1}), when protonation can lead to the formation of an ion-dipole complex $[CHCl_2\cdots HCl]^+$ unlike the protonation of chloro and dichloromethane. This complex is not the same as the ion-dipole complex $[CHCl_2\cdots OH_2]^+$ formed with the elimination of HCl in the proton transfer reaction between H_3O^+ and chloroform (discussed above).

Our experiments were conducted at 360 K and hence we also calculated the energy, free energy, and entropy of chloroform and dichloromethanol in their neutral and protonated forms to deter-

Table 3
Calculated G3 energy, free energy and entropy of protonated and neutral chloroform and dichloromethanol and the corresponding proton affinity (PA), entropy of protonation and gas-phase basicity (GB) of the neutral species at $T = 360$ and *298 K*.

Species	Energy (hartrees) 360 K *298 K*	Free Energy (hartrees) 360 K *298 K*	Entropy (cal mol^{-1} K^{-1}) 360 K *298 K*	PA (kcal mol^{-1}) 360 K *298 K*	$\Delta S_{1/2}$ (cal mol^{-1} K^{-1}) 360 K *298 K*	GB (kcal mol^{-1}) 360 K *298 K*
$CHCl_3$	−1418.822967 *−1418.824384*	−1418.864116 *−1418.857000*	73.7 *70.7*	157.4 *157.8*	20.9 *19.9*	155.2 *156.0*
$CH_2Cl_3^+$	−1419.071000 *−1419.073518*	−1419.124751 *−1419.115620*	94.6 *90.6*			
$CHCl_2OH$	−1034.558092 *−1034.559599*	−1034.599670 *−1034.592485*	74.5 *71.2*	163.5 *163.3*	2.6 *2.2*	154.7 *156.2*
$CH_2Cl_2OH^+$	−1034.815739 *−1034.817465*	−1034.858815 *−1034.851397*	77.1 *73.4*			

The gas phase basicity GB = PA + $T[\Delta S^T{}_{1/2} - S^T(H^+)]$, where $[\Delta S^T{}_{1/2}$ is the entropy difference between protonated and neutral species at T Kelvin, and $S_o{}^T(H^+)$ is the gas phase entropy of the hydrogen ion. $S^{360}(H^+) = 26.9$ cal K^{-1} mol^{-1} and $S^{298}(H^+) = 26.0$ cal K^{-1} mol^{-1} calculated from the Sackur–Tetrode equation.

mine their PAs and GBs at this temperature and compared them with our results at 298 K in Table 3. Our calculation of the entropy of chloroform at 298 K (70.7 cal mol^{-1} K^{-1}) is in excellent agreement with the NIST value (70.7 cal mol^{-1} K^{-1}) [40,51]. Differences between the gas phase basicities of $CHCl_3$ and $CHCl_2OH$ at 360 K and 298 K are small; ∼0.5 kcal mol^{-1} at 360 K and ∼0.2 kcal mol^{-1} at 298 K.

Our calculated PAs of CH_3Cl and for CH_2Cl_2 are within 0.4 kcal mol^{-1} of reported calculated values [39–42] and within 0.1 kcal mol^{-1} of calculations of the latest results reported by He and Wang [49] except for a discrepancy of 2.4 kcal mol^{-1} for CH_2Cl_2 between our results and a DFT calculation of the PA using the B3LYP approximation by Cacace et al. [56]. We believe our calculations of PAs at the G2 and G3 levels are more accurate than the DFT calculations. He and Wang's [49] calculations of the PAs of CH_3Cl, CH_2Cl_2, and $CHCl_3$ are, like Ma's [39], at the G3 level, except that the geometries were optimized using the B3LYP/6-31G(2df,p) functional and basis set and the zero point energy was obtained from the corresponding frequencies scaled by 0.9854. We used the standard G3 procedure [45] with the zero point energy corrected by using the HF frequency scaled by 0.8929, while Ma apparently used the MP2 frequencies scaled by 0.9661.

However, our calculations (also Ma et al. [39] and He and Wang's [49]) of the PAs of the chloromethanes at 298 K are significantly higher than the numbers quoted by Hunt and Andrews [57] and Holmes and Sodeau [58] who assumed a linear relationship between the frequency shift of the IR absorption (HF or D_2O) bands for the entire chloromethane series (cold trapped in solid argon matrices with either HF, DF [57] or D_2O [58] guest proton donor molecules) and the proton affinity (151.1 kcal mol^{-1} *vs.* 143 kcal mol^{-1} [57] for CH_2Cl_2 and 157.8 kcal mol^{-1} *vs.* 133 kcal mol^{-1} [57] for $CHCl_3$). Hunt and Andrews' estimate of the PA of CCl_4 as 130 kcal mol^{-1} is significantly lower than the G3 value of 167.2 kcal mol^{-1} calculated by Ma *et al.* and also our PA estimate based on Hess law principles. The examination by us of the frequencies of the ν_5 and ν_σ IR absorption bands of HF [57] and reported frequency shifts of the D_2O absorption band [58] *vs.* the available G3 calculated PA values (from this work and Refs. [39,49]) for CH_2Cl_2, $CHCl_3$, and CCl_4 (*i.e.*, excluding the CH_3Cl) showed excellent linear coefficient of > 0.9 for the frequency shift as a function of PA (the linear coefficient is drastically reduced by including CH_3Cl). Hunt and Andrews ignored the possibility of bidentate hydrogen bonding of the H atom in HF by 2 chlorine atoms in the chloromethanes containing 2, 3, or 4 chlorine substituents in their PA estimation based on IR frequency shifts. Using linear regression on the IR data (ν_σ and ν_5 bands) reported by Hunt and Andrews and the Ma et al. 298 G3 PA results for CH_2Cl_2, $CHCl_3$, and CCl_4 yielded the approximate relationship of PA ≈ $0.197\nu - 596$ kcal mol^{-1} with a reduced linear coefficient of ∼0.85, where ν is IR frequency in cm^{-1}; when applied to CH_3Cl this equations yields a very low PA value for CH_3Cl of ∼135 kcal mol^{-1} compared to the G3 value of 155 kcal mol^{-1} by Ma et al. The formation of the bidentate H bond induces a ∼100 cm^{-1} decrease in the IR frequency compared to a more modest ∼5 cm^{-1} increase per 1 kcal mol^{-1} increase in PA which shows that IR frequency shifts due to the formation of a dipole-dipole bifurcated H bond is a very significant factor if the variation in PAs is relatively small as in the case of the chloromethanes (150–170 kcal mol^{-1}). We suggest that chloromethanes with two or more chlorine substituents can better solvate the donor HF or D_2O compared to methylchloride by the formation of a bi/trifurcated hydrogen bonding between the two chlorine substituents of polychloromethanes and the donor D of D_2O [58] or H (or D) of HF (or DF) [57].

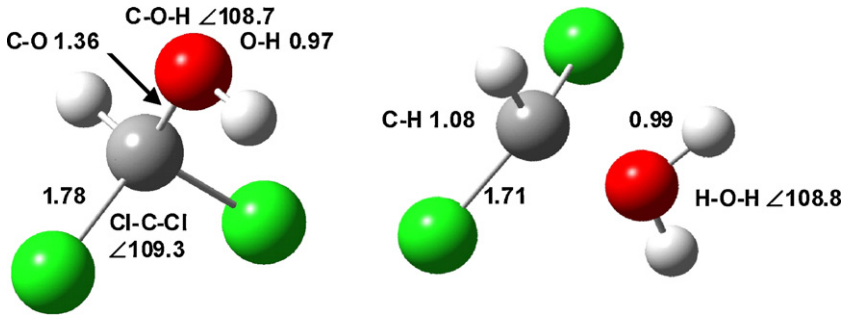

Fig. 4. MP2 (full)/6-31G (d) optimized structures of neutral and protonated dichloromethanol (protonation by bare proton) which exists as an ion-dipole complex (bond lengths and bond angles {∠} are given in ångströms and in degrees, respectively).

We observed that the protonation of dichloromethanol by a bare proton occurs preferentially on the hydroxyl oxygen. Interestingly, the structure of the resulting protonated dichloromethanol ion is a complex formed between dichloromethyl cation ($CHCl_2^+$) and a neutral water (H_2O) molecule with an elongated C–O bond distance of 1.57 Å (compared to ~1.37 Å in the neutral dichloromethanol which is in excellent agreement with the MP2 *ab initio* results of Anagnostou et al. [59] and the DFT results of Sun and Bozzelli [60]. A potential source of $CHCl_2^+$ could be from blackbody infrared radiative dissociation of parent ions in the ICR cell [50]. The optimized structures of neutral and protonated species of dichloromethanol (MP2 (full)/6-31+G (d, p)) are shown in Fig. 4.

The calculated PA (from G3) of 163.3 kcal mol^{-1} for dichloromethanol ($CHCl_2OH$) at 298 K is slightly lower than the experimental PA of water (PA = 165.0 kcal mol^{-1}). The gas phase basicity of dichloromathanol is significantly lower than its proton affinity (*e.g.*, at 360 K (*e.g.*, it is lower by 163.5 – 154.7 = 8.8 kcal mol^{-1}). This is due to the large negative entropy change for the protonation of dichloromethanol (−24.3 cal K^{-1} mol^{-1} at 360 K) which is the difference between the loss (−26.9 cal K^{-1} mol^{-1}) in entropy of the free hydrogen ion and the gain in entropy (2.6 cal K^{-1} mol^{-1}) of dichloromethanol on protonation when it forms an ion-dipole complex (Fig. 4). The entropy change will be larger when the complex dissociates. The circumstances in which entropy effects are important in gas phase (ion-molecule) reactions has been discussed by Irikura [61] and Meot-Ner [33].

At room temperature and in the absence of an activation barrier, the estimated Arrhenius PT reaction efficiency ($k/k_{Lg} = \exp\{-1.7\ \text{kcal mol}^{-1}/RT\}$) is about 0.06 (based on ΔPA). Under our experimental conditions, if dichloromethanol were eluted from the GC column, we should be able to observe its protonated form from reacting with the H_3O^+ reagent ion.

The above results confirm that the unknown species in our experimental samples with $m/z = 100.9$ formally corresponds to protonated dichloromethanol. The theoretical calculations confirm that the treated water samples are unlikely to contain dichloromethanol. However, protonated dichloromethanol $CHCl_2OH_2^+$ can be formed in several different ways (please refer to schemes I–III), one of which is through the formation of a proton bound heterodimer between chloroform ($CHCl_3$) and water, followed by the elimination of HCl. The energetics of this reaction is discussed below.

Protonation of chloroform by a bare proton at a chlorine atom also produces an ion-dipole complex but with an unusually long bond length of 3.12 Å (compared to ~1.6 Å for a normal C–Cl bond length) between the chlorine atom of the HCl dipole and the carbon atom of $CHCl_2^+$ ion as shown by *ab initio* calculations on protonated chloromethanes by Ma et al. [39] and independently by us. The PA of chloroform protonated at the most favorable site (*i.e.*, on chlorine) is 157.8 kcal mol^{-1} at 298 K. Structures of the protonated chloroform and hydronium-chloroform complex are shown in Fig. 5a and b, respectively.

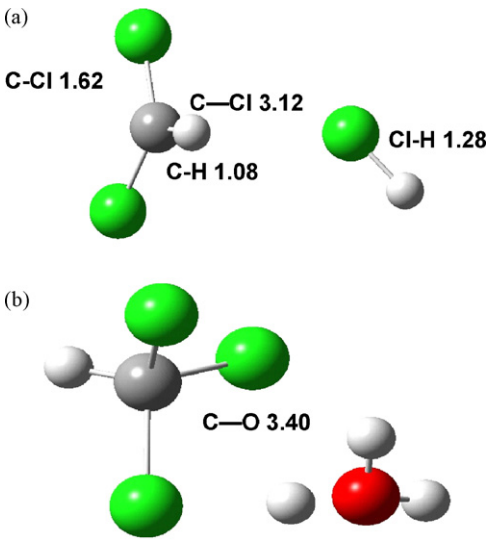

Fig. 5. (a) MP2 (full)/6-31G (d) optimized structures of protonated chloroform (protonation by bare proton) which exists as an ion-dipole complex. The equilibrium distance between the carbon atom and chlorine of the HCl dipole is 3.12 Å. (b) MP2/6-31+G** optimized structures of chloroform and protonated water which exists as a proton bound heterodimer. The equilibrium distance R(C–O) = 3.40 Å.

Although the entropy change for protonation of small molecules (*e.g.*, oxygenated compounds such as simple ketones [21]) is usually small, there is a large entropy contribution to the free energy of protonation of chloroform by a hydrogen ion to form an ion-dipole complex. The entropy difference $\Delta S^T_{1/2}$~21 cal mol^{-1} K^{-1} between protonated and unprotonated chloroform at 360 K is ~8 times larger than the corresponding difference for dichloromethanol (Table 3). This is largely due to the creation of three new low frequency scaled vibrations (at 40, 47, and 62 cm^{-1} resulting in an estimated $\Delta S_{1/2(\text{vib})}$ contribution of 16.4 cal mol^{-1} K^{-1}) and a large increase in the center of mass rotational moment of inertia ($\Delta S_{1/2(\text{rot})}$ contribution of 3.6 cal mol^{-1} K^{-1}) upon protonation of chloroform; the remaining 1 cal mol^{-1} K^{-1} is from all other degrees of freedom. The carbon chlorine bond at the chlorine protonation site is much longer in the ion-dipole complex of protonated

Table 4
Summary of G2 level calculations of reaction energies in kcal mol^{-1}.

Reaction	ΔE_{r298}	ΔH_{r298}	ΔH_r(expt)
$CHCl_3 + H_3O^+ \rightarrow [CHCl_2\cdots OH_2]^+ + HCl$	−5.4	−4.7	
$CHCl_3 + H_3O^+ \rightarrow CHCl_2^+ + H_2O + HCl$	11.2	11.8	13.9[a]
$CHCl_3 + H_3O^+ \rightarrow [CHCl_3\cdots H_3O]^+$	−18.8	−18.6	
$[CHCl_3\cdots H_3O]^+ \rightarrow [CHCl_2\cdots OH_2]^+ + HCl$	13.3		
$CHCl_2^+ + H_2O \rightarrow [CHCl_2\cdots OH_2]^+$	−15.9	−16.5	
	(−19.6)	(−17.1)	
$[CHCl_2\cdots OH_2]^+ \rightarrow CHClOH^+ + HCl$	−4.4	−3.8	
$H_3O^+ + H_2O \rightarrow H_5O_2^+$	−34.7	−35.2	−32.0 ± 2.0[a]
	(−35.9)	−33.4[b]	−32.0[c]
	(−34.4)[c]		

Numbers in parenthesis are from *ab initio* MP2/6-31+G** calculations.
[a] Experimental values from Ref. [51].
[b] From Ref. [70].
[c] From Ref. [63].

chloroform (3.12 Å for the complex *vs.* 1.57 Å for the neutral chloroform). The increase in entropy is largely compensated by the loss in entropy (−26.9 cal mol^{-1} K^{-1} at 360 K) of the hydrogen ion and hence the $GB_{360\,K}$ of chloroform is smaller than its PA by only ∼2 kcal mol^{-1}.

To investigate the origin of the unresolved peak in our mass spectrum, we carried out calculations of the energy changes for several ion-molecule reactions which form species of m/z = 100.9. A summary of our theoretical *ab initio* calculations are presented in Table 4.

All of the entries in Table 4, except the reactions listed in last two rows, give pathways for the formation of the ion-dipole complex $[CHCl_2\cdots OH_2]^+$. One is the direct elimination of HCl from the reaction of chloroform with protonated water as shown in row 1 of Table 4.

$$CHCl_3 + H_3O^+ \rightarrow [CHCl_2\cdots OH_2]^+ + HCl$$

This reaction energy calculated at the G2 level is exothermic by ∼5.4 kcal mol^{-1}. Another possible pathway is the condensation reaction of chloroform with protonated water to form a heterodimer [48] as shown in row 3 of Table 4, followed by HCl elimination to form an ion-dipole complex as in row 4 of Table 4.

$$CHCl_3 + H_3O^+ \rightarrow [CHCl_3\cdots H_3O]^+ \rightarrow [CHCl_2\cdots OH_2]^+ + HCl$$

The first reaction is exothermic by 18.8 kcal mol^{-1}, and the second is endothermic by 13.3 kcal mol^{-1}; both determined at the G2 level. The elimination of HCl from the complex requires breaking of two bonds; one is the H–O bond and the other is the C–Cl bond. Still another possible pathway is the association reaction of $CHCl_2^+$ fragment ions (see Figs. 1b and 3b) and background water to form $[CHCl_2\cdots H_2O]^+$ as in row 5 of Table 4.

$$CHCl_2^+ + H_2O \rightarrow [CHCl_2\cdots OH_2]^+$$

The reaction is calculated at the G2 level to be exothermic by 15.9 kcal mol^{-1}. In our experiments, we also observed two other species with m/z = 64.9785 (*i.e.*, CH_2ClO^+) and m/z = 37.0288 (*i.e.*, $H_5O_2^+$ with theoretical mass of 37.0284). The species at m/z = 64.9785 (*i.e.*, CH_2ClO^+) contains only one chlorine atom and is most likely formed by HCl elimination from the ion-dipole complex of $[CHCl_2\cdots H_2O]^+$ [55,62]. The enthalpy change for this reaction as shown in row 6 of Table 4 at G2 level is exothermic by 4.4 kcal mol^{-1}.

$$[CHCl_2\cdots OH_2]^+ \rightarrow CHClOH^+ + HCl$$

This confirms that the unknown species of m/z = 100.9 (*i.e.*, $CH_3OCl_2)^+$ originated from chloroform which was present in the treated water samples as well as our control water sample containing the added authentic chloroform standard.

Returning to the formation of the ion-dipole complex in the proton transfer reaction from H_3O^+ to chloroform, as noted earlier, the dissociation of the ion-dipole complex makes the entropy change more positive. The overall reaction for proton transfer with dissociation is

$$CHCl_3 + H_3O^+ \rightarrow CHCl_2^+ + H_2O + HCl$$

The enthalpy change ΔH for this reaction is the difference between the proton affinities of water (165.0 kcal mol^{-1}) and chloroform (157.8 kcal mol^{-1}) plus the bond dissociation energy of the complex, which [49] is 25 kJ mol^{-1} or approximately 6 kcal mol^{-1}. It follows that ΔH = 13.2 kcal mol^{-1} and the proton transfer reaction is endothermic. The entropies of $CHCl_3$, H_3O^+, H_2O and HCl at 298 K are 70.7, 46.1, 45.1 and 44.7 cal mol^{-1} K^{-1}, respectively from standard tables (NIST) [40]. We have calculated the entropy of $CHCl_2^+$ at the G2 level to be 64.5 cal mol^{-1} K^{-1} at 298 K (*cf.* 64.1 cal mol^{-1} K^{-1} at 298 K [40] for the isoelectronic analog, $BHCl_2$) and it follows that the entropy change ΔS for this reaction at 298 K is 37.5 cal mol^{-1} K^{-1}. The corresponding free energy ($\Delta G_T = \Delta H - T\Delta S$) at 298 K, ΔG_{298} = 2.0 kcal mol^{-1}, and proton transfer is unfavorable. Assuming that ΔH and ΔS remain unchanged or are nearly the same at 360 K as at 298 K, the free energy change at 360 K, ΔG_{360} = −0.3 kcal mol^{-1}. Proton transfer from protonated water to chloroform is exoergic and thus favorable at 360 K and entropically driven at the temperature of our experiment [33,61].

As noted above, $H_5O_2^+$ (or $(H_2O)_2H^+$) was also present in our mass spectrum; we studied the reaction between protonated and neutral water to form $H_5O_2^+$:

$$H_3O^+ + H_2O \rightarrow H_5O_2^+$$

This reaction is exothermic by 34.7 kcal mol^{-1} (row 7 of Table 4) [63]. The $H_5O_2^+$ is a proton bound water dimer and is probably the Zundel structure [64] proposed as an intermediate in proton transfer in liquid water [65]. The experimentally measured mass of 37.0288 agrees with the theoretical value (37.0284) for the mass of $H_5O_2^+$. The formation of $H_5O_2^+$ either by bimolecular ion-molecule radiative association reaction ($H_3O^+ + H_2O \rightarrow H_5O_2^+ + h\nu$) [66] or termolecular reaction in the presence of He buffer gas ($H_3O^+ + H_2O + He \rightarrow H_5O_2^+ + He$) [67,68] are extremely inefficient processes under our GC/FT-ICR MS conditions. For example, at an estimated peak He pressure of ∼10^{-4} Torr (based on our previous experimental measurements [21]) and background water pressure of <10^{-8} Torr in the ICR cell, the time constant for the ter-body reaction ($H_3O^+ + H_2O + He \rightarrow H_5O_2^+ + He$) would be >1 Ms using the ter-body rate constants (∼10^{-27} cm^6 molecules^{-2} s^{-1}) [67,68]. However, there might be sufficient number of collisions with He carrier gas and other water molecules in the cell, as well as the collisions with eluting chloroform to cool and stabilize the initially formed excited proton bound heterodimer of water and chloroform (not observed in our experiments, but observed by SIFT MS [48]) which subsequently ligand exchanges with background water to yield $H_5O_2^+$ at m/z = 37.0284 in our GC/FT-ICR MS experiments. The $H_5O_2^+$ species is only observed when $CHCl_3$ elutes off the GC in CI/GC/FT-ICR MS experiments and H_2O is one of the CI reagents and not in EI/GC/FT-ICR MS type experiments. The formation of the protonated dimer ($H_5O_2^+$) has been observed in FT-ICR mass spectrometry studies of 1,1,3,3-tetrafluorodimethylether (TFDE) in bimolecular reactions [69]. In addition, we do not believe that the pressure in our ICR cell ever approaches that of a SIFT experiment of ∼0.5–1 Torr for the formation of $H_5O_2^+$ by a ter-body association mechanism to be effective. Previously, we reported that it takes >1.5 s per decade of pressure decay for the pressure of He in the ICR cell after the GC introduction event to decay from an estimated peak pressure of 10^{-4} Torr [21]. Even if hypothetically the pressure in the ICR cell reached 1 Torr (highly impossible for our GC flow rate of <1 sccm), it would take >12 s to attain a pressure of <10^{-8} Torr for marginal FT-ICR MS operation; our reaction time delays between the GC introduction and the detection events in our GC/FT-ICR-MS experiments were only ∼8 s.

5. Conclusions

The combined use of experimental GC/FT-ICR mass spectrometry data and high level *ab initio* calculations of energies, proton affinities, and gas phase basicities allow deciphering important competing pathways for proton transfer, “dissociative proton attachment (DPA)”, and condensation reactions to improve unknown identification. Direct *ab initio* calculations of proton affinities of chloromethanes and chloromethanols were carried at the G3 levels at 298 K and the proton affinities and gas

phase and basicities of chloroform dichloromethanol were calculated at the experimental temperature of 360 K and at 298 K. The change in proton affinity of chloroform from 298 to 360 K was less than 0.4 kcal mol^{-1} and the gas phase basicity changed by ~0.8 kcal mol^{-1}. Detailed investigations of possible ion-molecule reactions reveal that the origin of CCl_3^+ ions (from EI experiments) and unknown species of m/z = 100.9 (*i.e.*, $[CH_3Cl_2O]^+$ in the CI experiments) is chloroform present in the treated water samples. Analysis of known water standard samples spiked with authentic chloroform under the identical experimental conditions confirmed our assignments.

The *ab initio* protonation studies of chloroform ($CHCl_3$) and dichloromethanol (Cl_2CHOH) at the G3 level show that PAs of these two compounds are lower than that of water. The G3 level calculations for $CHCl_3$ and $CHCl_2OH$ yielded PA values of 157.8 kcal mol^{-1} and 163.3 kcal mol^{-1}, respectively at 298 K in contrast to the PA of water which is 165 kcal mol^{-1}. The protonation of chloroform by H_3O^+ to form $CHCl_2^+$, H_2O and HCl is energetically unfavorable (ΔH = 13.2 kcal mol^{-1}) but entropically favored by 37.5 cal mol^{-1} K^{-1}. Although the free energy change for this reaction is positive at 298 K, it is negative at 360 K, showing that proton transfer from H_3O^+ to chloroform is entropically driven at the experimental temperature of 360 K.

We conclude that the species $(CH_3Cl_2O)^+$ at m/z = 100.9 observed in mass spectrum of water samples is not dichloromethanol; but an ion-molecule complex $(CHCl_2\cdots OH_2)^+$ formed either by HCl elimination when chloroform reacts with protonated water or by the association of the fragment ion $CHCl_2^+$ from chloroform and background water. The appearance of $H_5O_2^+$ ion (*i.e.*, Zundel cation) in our mass spectrometer is uncommon and we speculate that the Zundel cation occurs *via* ion-molecule reactions of GC eluted analytes in the presence of He carrier gas.

Acknowledgments

We thank the referees for their incisive comments and are grateful to them for calling our attention to the papers by Hunt and Andrews and Irikura. This project was funded by the Maine Water Resources Research Institute with support and collaboration of the Department of the Interior, U.S. Geological Survey and the University of Maine (Grant No. 01HQGR0083). Financial support from NSF (Award No. 0228971 for instrument development) and Department of Defense (CDMRP-OC060322) is also gratefully acknowledged. JCR and IS were supported by a grant from the NSF (CHE 0549187). The views and conclusions contained herein are entirely the responsibility of the authors and should not be interpreted as necessarily representing the official policies, or endorsements, either expressed or implied, of the funding agencies or U.S. Government. The authors thank John Peckenham for providing water samples and valuable discussions.

References

[1] S.D. Richardson, A.D. Thruston Jr., T.W. Collette, K.S. Patterson, B.W. Lykins Jr., J.C. Ireland, Identification of TiO_2/UV disinfection byproducts in drinking water, Environ. Sci. Technol. 30 (1996) 3327–3334.
[2] S.D. Richardson, A.D. Thruston Jr., T.V. Caughran, P.H. Chen, T.W. Collette, T.L. Floyd, K.M. Schenck, B.W. Lykins Jr., G.-r. Sun, G. Majetich, Identification of new drinking water disinfection byproducts formed in the presence of bromide, Environ. Sci. Technol. 33 (1999) 3378–3383.
[3] S.W. Krasner, H.S. Weinberg, S.D. Richardson, S.J. Pastor, R. Chinn, M.J. Sclimenti, G.D. Onstad, A.D. Thruston, Occurrence of a new generation of disinfection byproducts, Environ. Sci. Technol. 40 (2006) 7175–7185.
[4] S.D. Richardson, The role of GC–MS and LC–MS in the discovery of drinking water disinfection byproducts, J. Environ. Monit. 4 (2002) 1–9.
[5] J.J. Rook, Formation of haloforms during chlorination of natural waters, Water Treat. Exam. 23 (1974) 234–243.
[6] H. Komulainen, V.M. Kosma, S.L. Vaittinen, T. Vartiainen, E. Kaliste-Korhonen, S. Lötjönen, R.K. Tuominen, J. Tuomisto, Carcinogenicity of the drinking water mutagen 3-chloro-4(dichloromethyl)-5-hydroxy-2(5h)-furanone in the rat, J. Natl. Cancer Inst. 89 (1997) 848–856.
[7] W.D. King, L.D. Marrett, C.G. Woolcott, Case-control study of colon and rectal cancers and chlorination byproducts in treated water, Cancer Epidemiol. Biomark. Prevent. 9 (2000) 813–818.
[8] M.T. Do, N.J. Birkett, K.C. Johnson, D. Krewski, P. Villeneuve, B. Paulse, R. Dewar, D. Dryer, N. Kreiger, E. Kliewer, D. Robson, S. Fincham, N. Le, Chlorination disinfection byproducts and pancreatic cancer risk, Environ. Health Perspect. 113 (2005) 418–424.
[9] M.J. Nieuwenhuijsen, M.B. Toledano, N.E. Eaton, J. Fawell, P. Elliott, Chlorination disinfection byproducts in water and their association with adverse reproductive outcomes: a review, Occup. Environ. Med. 57 (2000) 73–85.
[10] J.M. Wright, J. Schwartz, D.W. Dockery, Effect of trihalomethane exposure on fetal development, Occup. Environ. Med. 60 (2003) 173–180.
[11] M.I. Cedergren, A.J. Selbing, O. Löfman, B.A.J. Källen, Chlorination byproducts and nitrate in drinking water and risk for congenital cardiac defects, Environ. Res. 89 (2002) 124–130.
[12] A. McCulloch, Chloroform in the environment: occurrence, sources, sinks and effects, Chemisphere 50 (2003) 1291–1308.
[13] S.D Richardson, Environmental mass spectrometry: emerging contaminants and current issues, Anal. Chem. 78 (2006) 4021–4046.
[14] V.Y. Taguchi, Structural elucidation of disinfection byproducts in treated drinking water, Rapid Commun. Mass Spectrom. 15 (2001) 455–461.
[15] T. Anspach, J. Efer, L. Wennrich, A. Schreiber, W. Engewald, LC–MS analysis of halogenated organic compounds formed by chlorination of water containing humic substances, Vom Wasser 94 (2000) 11–28.
[16] C. Zwiener, S.D. Richardson, Analysis of disinfection byproducts in drinking water by LC–MS and related MS techniques, Trends Anal. Chem. 24 (2005) 613–621.
[17] C. Zwiener, T. Glauner, F.H. Frimmel, LC-ESI/MS/MS analysis with derivatization applied to polar disinfection byproducts in water treatment, Water Sci. Technol. Water Supply 3 (2003) 321–328.
[18] T. Solouki, J.E. Szulejko, I. Silwal, C. Heffner, Experimental and theoretical approaches: identification of disinfection byproducts in drinking water with multidimensional GC/FT-ICR MS, in: Proceedings of the 54th ASMS Conference on Mass Spectrometry and Allied Topics, Seattle, WA, 2006.
[19] C. Heffner, I. Silwal, J.M. Peckenham, T. Solouki, Emerging technologies for identification of disinfection byproducts: GC/FT-ICR MS characterization of solvent artifacts, Environ. Sci. Technol. 41 (2007) 5419–5425.
[20] J.-Y. Salpin, M. Mormann, J. Tortajada, M.-T. Nguyen, D. Kuck, The gas-phase basicity and proton affinity of 1,3,5-cycloheptatriene—energetics, structure and interconversion of dihydrotropylium ions, Eur. J. Mass Spectrom. 9 (2003) 361–376.
[21] J.E. Szulejko, Z. Luo, T. Solouki, Simultaneous determination of analyte concentrations, gas-phase basicities, and proton transfer kinetics using gas chromatography/Fourier transform ion cyclotron resonance mass spectrometry (GC/FT-ICR MS), Int. J. Mass Spectrom. 257 (2006) 16–26.
[22] Z. Luo, C. Heffner, T. Solouki, Multidimensional GC-Fourier transform ion cyclotron resonance MS analyses: utilizing gas-phase basicities to characterize multicomponent gasoline samples, J. Chromatogr. Sci. 47 (2009) 75–82.
[23] C.W. Polley Jr., B. Munson, Quantitation by reactant ion monitoring in gas chromatography/chemical ionization mass spectrometry, Anal. Chem. 53 (1981) 308–312.
[24] V.T. Tran, B. Munson, Proton affinities by reactant ion monitoring: triphenyl group Va compounds, Org. Mass Spectrom. 21 (1986) 41–46.
[25] C.B. Jacoby Jr., D. Rempel, M.L.A. Gross, Cold trap/pulsed valve GC/FTMS interface: ultra-trace analysis, in: Proceedings of the 38th ASMS Conference on Mass Spectrometry and Allied Topics, Tucson, AZ, 1990.
[26] J. Bennett, Improvements to PC/GC FT-ICR mass spectrometry performance [Honors Thesis]. University of Maine, ME, Orono, 2003.
[27] M. Chai, C.L. Arthur, J. Pawliszyn, R.P. Belardi, K.F. Pratt, Determination of volatile chlorinated hydrocarbons in air and water with solid-phase microextraction, Analyst 118 (1993) 1501–1505.
[28] F.J. Santos, M.T. Galceran, D. Fraisse, Application of solid-phase microextraction to the analysis of volatile organic compounds in water, J. Chromatogr. A 742 (1996) 181–189.
[29] P.B. Grosshans, A.G. Marshall, General-theory of excitation in ion-cyclotron resonance mass-spectrometry, Anal. Chem. 63 (1991) 2057–2061.
[30] S.H. Guan, A.G. Marshall, Stored wave-form inverse Fourier-transform axial excitation/ejection for quadrupole ion-trap mass-spectrometry, Anal. Chem. 65 (1993) 1288–1294.
[31] E. de Hoffmann, J. Charette, V. Stroobant, Mass Spectrometry: Principles and Applications, John Wiley & Sons, New York, 1994.
[32] L.A. Curtiss, K. Raghavachari, G.W. Trucks, J.A. Pople, Gaussian-2 theory for molecular energies of first- and second-row compounds, J. Chem. Phys. 94 (1991) 7221–7230.
[33] M. Meot-Ner, Entropy-driven proton-transfer reactions, J. Phys. Chem. 95 (1991) 6580–6585.
[34] G. Bouchoux, J.Y. Salpin, D. Leblanc, A relationship between the kinetics and thermochemistry of proton transfer reactions in the gas phase, Int. J. Mass Spectrom. Ion Proc. 153 (1996) 37–48.
[35] M.J. Frisch, G.W. Trucks, H.B. Schlegel, G.E. Scuseria, M.A. Robb, J.R. Cheeseman, J.A. Montgomery Jr., T. Vreven, K.N. Kudin, J.C. Burant, J.M. Millam, S.S. Iyengar, J. Tomasi, V. Barone, B. Mennucci, M. Cossi, G. Scalmani, N. Rega, G.A. Petersson,

H. Nakatsuji, M. Hada, M. Ehara, K. Toyota, R. Fukuda, J. Hasegawa, M. Ishida, T. Nakajima, Y. Honda, O. Kitao, H. Nakai, M. Klene, X. Li, J.E. Knox, H.P. Hratchian, J.B. Cross, C. Adamo, J. Jaramillo, R. Gomperts, R.E. Stratmann, O. Yazyev, A.J. Austin, R. Cammi, C. Pomelli, J.W. Ochterski, P.Y. Ayala, K. Morokuma, G.A. Voth, P. Salvador, J.J. Dannenberg, V.G. Zakrzewski, S. Dapprich, A.D. Daniels, M.C. Strain, O. Farkas, D.K. Malick, A.D. Rabuck, K. Raghavachari, J.B. Foresman, J.V. Ortiz, Q. Cui, A.G. Baboul, S. Clifford, J. Cioslowski, B.B. Stefanov, G. Liu, A. Liashenko, P. Piskorz, I. Komaromi, R.L. Martin, D.J. Fox, T. Keith, M.A. Al-Laham, C.Y. Peng, A. Nanayakkara, M. Challacombe, P.M.W. Gill, B. Johnson, W. Chen, M.W. Wong, C. Gonzalez, J.A. Pople, Gaussian 03, Revision c.02, Gaussian, Inc., Wallingford, CT, 2004.

[36] L.A. Curtiss, P.C. Redfern, V. Rassolov, J.A. Pople, Gaussian-3 (G3) theory for molecules containing first and second-row atoms, J. Chem. Phys. 109 (1998) 7764–7776.

[37] K.K. Irikura, R.D. Johnson III, R.N. Kacker, Uncertainties in scaling factors for ab initio vibrational frequencies, J. Phys. Chem. A 109 (2005) 8430–8437.

[38] J.P. Merrick, D. Moran, L. Radom, An evaluation of harmonic vibrational frequency scale factors, J. Phys. Chem. A 111 (2007) 11683–11700.

[39] N.L. Ma, K.C. Lau, S.H. Chien, W.K. Li, Thermochemistry of hydrochlorofluoromethanes revisited: a theoretical study with the Gaussian-3 (G3) procedure, Chem. Phys. Lett. 311 (1999) 275–280.

[40] E.P. Hunter, S.G. Lias, P.J. Linstrom, W.G. Mallard, Evaluated gas phase basicities and proton affinities of molecules: an update, J. Phys. Chem. Ref. Data 27 (1998) 413–656.

[41] C. Adhart, O. Sekiguchi, E. Uggerud, On the gas-phase reactivity of complexed OH^+ with halogenated alkanes, Chem. Eur. J. 11 (2004) 152–159.

[42] M.N. Glukhovtsev, J.E. Szulejko, T.B. McMahon, J.W. Gauld, A.P. Scott, B.J. Smith, A. Pross, L. Radom, New theoretical and experimental proton affinities for methyl halides and diazomethane—a revision of the methyl cation affinity scale, J. Phys. Chem. 98 (1994) 13099–13101.

[43] J.A. Pople, M. Head-Gordon, D.J. Fox, K. Raghavachari, L.A. Curtiss, Gaussian-1 theory: a general procedure for prediction of molecular energies, J. Chem. Phys. 90 (1989) 5622–5629.

[44] L.A. Curtiss, P.C. Redfern, K. Raghavachari, J.A. Pople, Assessment of Gaussian-2 and density functional theories for the computation of ionization potentials and electron affinities, J. Chem. Phys. 109 (1998) 42–55.

[45] J.B. Foresman, A. Frish, Exploring Chemistry with Electronic Structure Methods, Gaussian, Inc., Pittsburgh, 1996.

[46] D.L. Phillips, C.Y. Zhao, D.Q. Wang, A theoretical study of the mechanism of the water-catalyzed HCl elimination reactions of CHXCl(OH) (X = H, Cl) and HClCO in the gas phase and in aqueous solution, J. Phys. Chem. A 109 (2005) 9653–9673.

[47] R.J. Silbey, R.A. Alberty, M.G. Bawendi, Physical Chemistry, fourth ed., John Wiley & Sons, Inc., New York, 2005.

[48] P. Španěl, D. Smith, Selected ion flow tube studies of the reactions of H_3O^+, NO^+, and O_2^+ with some chloroalkanes and chloroalkenes, Int. J. Mass Spectrom. 184 (1999) 175–181.

[49] Y.-L. He, L. Wang, Potential energy surfaces for protonation of hydrochlorofluoromethanes, J. Mol. Struct. Theochem 913 (2009) 240–246.

[50] T. Solouki, J.E. Szulejko, Bimolecular and unimolecular contributions to the disparate self-chemical ionizations of α-pinene and camphene isomers, J. Am. Soc. Mass Spectrom. 18 (2007) 2026–2039.

[51] P.J. Linstrom, W.G. Mallard (Eds.), Proton affinity evaluation in NIST chemistry webbook, NIST standard reference database number 69 [database on the Internet], 2009. Available from: http://webbook.nist.gov/chemistry/.

[52] [a] J.E. Szulejko (unpublished results, available upon request from J. E. Szulejko), High Pressure MS (HPMS) association reaction thermochemical data (for the period 1987 to September 1998, pp. 1–9), obtained in the laboratory of Professor T. B. McMahon, University of Waterloo, Canada;
[b] R.G. Keesee, A.W. Castleman Jr., Thermochemical data on gas-phase ion-molecule association and clustering reactions, J. Phys. Chem. Ref. Data 15 (1986) 1011–1071.

[53] R. Mabrouki, Y. Ibrahim, E. Xie, M. Meot-Ner, M.S. El-Shall, Gas phase hydration and deprotonation of the cyclic $C_3H_3^+$ cation. Solvation by acetonitrile, and comparison with the benzene radical cation, J. Phys. Chem. A 110 (2006) 7334–7344.

[54] L. Wang, J. Zhang, Quantum chemistry study on cation structures of fluorinated and chlorinated germanes and their radicals, J. Phys. Chem. A 112 (2008) 3454–3465.

[55] E. Marotta, G. Scorrano, C. Paradisi, Ionic reactions of chlorinated volatile organic compounds in air plasma at atmospheric pressure, Plasma Process. Polym. 2 (2005) 209–217.

[56] F. Cacace, G. de Petris, F. Pepi, M. Rosi, A. Troiani, Gaseous $[H_3C–Cl–Cl]^+$ ions from the reaction of methane with Cl_3^+, the first example of a new dihalogenation process: formation and characterization of $CH_3Cl_2^+$ isomers by experimental and theoretical methods, Chem. Eur. J. 5 (1999) 2750–2756.

[57] R.D. Hunt, L. Andrews, Infrared spectra of HF complexes with CCl_4, $CHCl_3$, and CH_2Cl_2 in solid argon, J. Phys. Chem. 96 (1992) 6945–6949.

[58] N.S. Holmes, J.R. Sodeau, A study of the interaction between halomethanes and water-ice, J. Phys. Chem. A 103 (1999) 4673–4679.

[59] F. Anagnostou, E. Drougas, A.M. Kosmas, Quantum mechanical analysis of decomposition pathways of chloromethyl hypochlorite, J. Mol. Struct. Theochem 728 (2005) 189–196.

[60] H. Sun, J.W. Bozzelli, Structures, intramolecular rotation barriers, and thermochemical properties of radicals derived from H atom loss in mono-, di-, and trichloromethanol and parent chloromethanols, J. Phys. Chem. A 105 (2001) 4504–4516.

[61] K.K. Irikura, The ionization energy of CF_3: when does entropy matter in gas-phase reactions? J. Am. Chem. Soc. 121 (1999) 7689–7695.

[62] P. Španěl, D. Smith, Selected ion flow tube studies of the reactions of H_3O^+, NO^+, and O_2^+ with several aromatic and aliphatic monosubstituted halocarbons, Int. J. Mass Spectrom. 189 (1999) 213–223.

[63] L. Ojamae, I. Shavitt, S.J. Singer, Potential models for simulations of the solvated proton in water, J. Chem. Phys. 109 (1998) 5547–5564.

[64] S. Woutersen, H.J. Bakker, Ultrafast vibrational and structural dynamics of the proton in liquid water, Phys. Rev. Lett. 96 (2006) 138305–138308.

[65] D. Mark, M. Tuckerman, J. Hutter, M. Parrinello, The nature of the hydrated excess proton in water, Nature 397 (1999) 601–604.

[66] P. Kofel, T.B. McMahon, Determination of radiative and unimolecular decomposition lifetimes of chemically activated ions by Fourier-transform ion-cyclotron resonance spectrometry, J. Phys. Chem. 92 (1988) 6174–6176.

[67] S. Hamon, T. Speck, J.B.A. Mitchell, B. Rowe, Experimental and modeling study of the ion-molecule association reaction $H_3O^+ + H_2O(+M) \rightarrow H_5O_2(+M)$, J. Chem. Phys. 123 (2005) 054303.

[68] J.S. Chang, D.M. Golden, Kinetics and thermodynamics for ion-molecule association reactions, J. Am. Chem. Soc. 103 (1981) 496–500.

[69] R.A. Marta, T.B. McMahon, T.D. Fridgen, Infrared multiphoton dissociation spectra as a probe of ion molecule reaction mechanism: the formation of the protonated water dimer via sequential bimolecular reactions with 1,1,3,3-tetrafluorodimethyl ether, J. Phys. Chem. A 111 (2007) 8792–8802.

[70] A. Likholyot, K.H. Lemke, J.K. Hovey, T.M. Seward, Mass spectrometric and quantum chemical determination of proton water clustering equilibria, Geochim. Cosmochim. Acta 71 (2007) 2436–2447.